RSC Advances

ROYAL SOCIETY OF CHEMISTRY

www.rsc.org/advances

RSCAdvances RSCPublishing

ARTICLE

Cite this: DOI: 10.1039/x0xx00000x

Received 00th January 2015,
Accepted 00th January 2015

DOI: 10.1039/x0xx00000x

www.rsc.org/

Silicon dioxide covered Au and Ag nanoparticles for Shell-Isolated Nanoparticles Enhanced Spectroscopies in the near-infrared

Tatiana B. V. Neves,[a] Sandra M. Landi,[b] Lídia A. Sena,[b] Bráulio S. Archanjo,[b] Gustavo F. S. Andrade,[a,*]

The present work reports the extension of the SHINERS and SHINEF (shell-isolated nanoparticles enhanced Raman scattering, and fluorescence, respectively) effects into the near-infrared excitation, at 1064 nm and 785 nm, respectively. The plasmon enhanced effects were obtained for the SHIN Au@SiO_2 and Ag@SiO_2 nanoparticles. The overall SHINERS performance of both SHIN in the presence of the probe dye IR-820 is considerably lower than for the visible region of the spectra, and the conjunction to the IR-820 dye has been essential for the observation of SHINERS. The SHINEF performance for both SHIN excited at 785 nm is quite similar; this similarity is assigned to the similar values of quality factor for the two coinage metals in that region of the electromagnetic spectrum.

1. Introduction

In recent years it has been reported in the literature an approach for the improvement of stability of silver and gold nanoparticles by the coverage with ultrathin layers of several oxides, resulting in coinage metals covered nanoparticles, M@XO_y.[1-4] The most widely used oxide has been silica, which introduced improved stability to the colloidal suspension as well as the possibility of using the nanoparticles as smart dust for detection of SERS signal from non-enhancing solid media.[5] The technique resulting from this coverage have been referred to as SHINERS (shell isolated nanoparticles enhanced Raman scattering).

Shortly after the proposition of SHINERS, the observation of surface-enhanced fluorescence on Ag@SiO_2 nanoparticles, named SHINEF (shell isolated nanoparticles enhanced fluorescence) was reported.[6] The enhancement phenomenon in SHINEF has been experimentally confirmed shortly after.[7, 8]

Both SHINERS and SHINEF have to take into account that the adsorbate will be kept away from the coinage metal surface with the thickening of ultrathin oxide layers,; this is an essential requirement for the enhanced fluorescence, but the decrease in SERS (surface-enhanced Raman scattering) intensities with distance from surface is very well documented.[9-11] The usefulness of SHINERS approach depends strongly on the possibility of controlling the silicon oxide thickness in the production of the shell isolated nanoparticles (SHIN). In the case of SHINEF, it is necessary to determining an optimized thickness for the SiO_2 layer, as to guarantee the necessary separation between conductive nanoparticles (Ag, Au or Cu) and the adsorbate to avoid fluorescence quenching; nevertheless the oxide layer cannot be so thick that the enhancement by the surface plasmon falls off, as for adsorbate distances longer than 10 nm.[12, 13] The correct compromise between distance of the coinage metal surface to the adsorbate may result in large fluorescence enhancement, and yet present interesting SERS performance in different spectral ranges.

It would be important extending both SHINERS and SHINEF further toward the near-infrared excitations, as those are the less damaging radiation for living tissues; additionally, longer wavelengths present deeper penetration through tissues, which are wanted characteristic for *in vivo* applications of both techniques. Specifically for SHINERS, there has been no report for this technique excited at 1064 nm, the exciting radiation for FT-Raman, which is a largely used Raman setup in several laboratories around the world. The performance for local field enhancement by localized-surface plasmon resonance decreases for the 1064 nm excitation, because the coinage metals nanoparticles resonant at this wavelength are so large that retardation effects may occur and decrease the dipole efficiency.[14] However, the compromise between the decreasing field localization and the important availability of FT-Raman systems results in growing interest in studying methodologies for the improvement of FT-Raman directed SERS/SHINERS substrates.[15] For such approach, it should be important to find a precise adsorbate that present a large intrinsic Raman scattering cross section in the near-infrared, so that the evaluation of the enhancement performance could be performed. A similar argument may be used for SHINEF, but an infrared fluorescent dye must be used as probe in such case.

One dye that may be used for both SHINERS and SHINEF effects in the near-infrared is IR-820 (structure presented in Scheme 1), a cyanine-type dye that fluoresces at *ca.* 820 nm, and presents a strong absorption band at 690 nm with a hot-band shoulder at 819 nm.[16] Due to this absorption band, IR-820 is pre-resonant in the 1064 nm, and may have fluorescence excited at 785 nm. Additionally, the SERS effect of IR-820 in Au and Ag nanoparticles has been studied recently.[16] Both fluorescence and SERS properties allowed this dye to be chosen as the probe for both SHINERS and SHINEF in the present work.

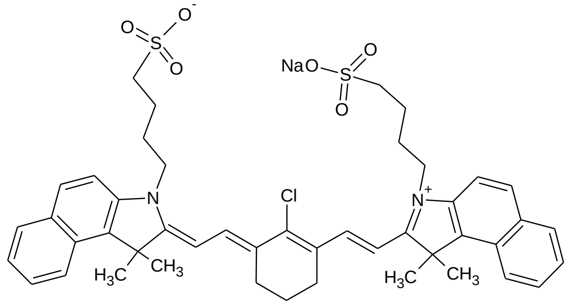

Scheme 1. Structure of IR-820.

In the present work, therefore, SHINERS and SHINEF spectra of the IR-820 dye excited at 1064 and 785 nm, respectively, are reported, both measured for the same set of Au@SiO_2 and Ag@SiO_2 nanoparticles. It is shown that both SHINERS and SHINEF may be obtained for the same substrates in two different wavelengths with performance similar to what has been observed when excited in the visible.

2. Experimental Section

2.1. Chemicals

Tetrachloroauric acid ($HAuCl_4$, 99%), silver nitrate (AgNO3, 99,99%), trisodium citrate (Na3-cit, 99%), potassium hydroxide (KOH, 85%), sodium silicate (Na_2SiO_4, 27% solution), (3-aminopropyl)-trimethoxysilane (APTMS, 97%) and IR-820 (80%) were all acquired from Sigma-Aldrich. All aqueous solutions have been prepared using deionized water (18.2 MΩ cm) from a deionizer Millipore, Synergy UV model.

2.2. Synthesis of Au and Ag nanoparticles

The gold and silver nanoparticles suspensions have been synthesized from the precursors $HAuCl_4$ and $AgNO_3$, respectively, in aqueous solution, following well known procedures from the literature.[17,18]

Briefly, gold nanoparticles (AuNP)[17] were prepared using 50 mL of an aqueous $HAuCl_4$ solution (0.01%m) under reflux to which 500 μL of an 1.0% Na_3-cit solution; the reflux was maintained for 10 min after addition of citrate. The resulting suspension was red, and typically presented extinction maxima with a maximum at 530 nm. Silver nanoparticles (AgNP)[18] suspensions were prepared bringing to reflux 100 mL of aqueous $AgNO_3$ (0.018%) and adding 2.0 mL of 1.0% Na_3-cit. The reflux was maintained for 1 h. The resulting solution was grey and presented an extinction maximum at 420 nm. Both nanoparticles suspensions were kept at 4°C for further use.

2.3. SiO_2 ultrathin film growth for shell-isolated nanoparticles (SHIN)

For the growth of ultrathin layers of silica over AgNP and AuNP, 400 μL of a 0.01 mol L^{-1} APTMS was added to 30 mL of nanoparticle suspension.[4] After surface modification, it was added 3200 μL of a 0.54% sodium silicate solution; the resulting solution was vigorously mixed, and then kept at 90°C in reflux for times ranging from 1 to 2.5 h.

2.4. Spectroscopy and microscopy measurements

The UV-VIS spectra were obtained in a spectrometer Shimadzu, model 1800 in the range of 200-1100 nm.

Transmission electron microscopy (TEM) was performed in a Cs probe-corrected FEI Titan 80-300 microscope operating at 300 kV, equipped with an energy dispersive X-ray (EDX) analyzer. Two techniques were applied: conventional diffraction contrast TEM and scanning transmission electron microscopy (STEM) using a high-angle annular dark-field (HAADF) detector. The samples were purified by 2 cycles of centrifugation/redispersion, being finally dispersed in deionized water and drop-casted directly on holey carbon TEM grids.

The SHINEF and regular fluorescence spectra were acquired in a Bruker spectrometer, model Senterra, with back-scattering collection. The excitation radiation was the laser line at 785 nm, with laser power at laser head of 1 mW. The laser was focused on the sample by a 50X magnification objective (NA=0.75), and the acquisition time was 25 s.

The SHINERS and normal Raman spectra were acquired in a FT-Raman spectrometer from Bruker, model RFS/100, excited at 1064 nm, and in 180° collection geometry. The laser power was 300 mW in the laser head. The samples were always prepared at least 24 h before measurement. IR-820 was always added from a solution 10 times more concentrated than the desired concentration.

3. Results and discussions

3.1. LSPR and TEM characterization of Ag@SiO_2 and Au@SiO_2

The growth of the silicon oxide layer over the nanoparticles results in a change in the refractive index of the dielectric medium in contact with the nanoparticles; so, it is expected a shift in the localised surface plasmon resonance (LSPR) bands of either AgNP or AuNP. Figure 1 presents the LSPR of AgNP and AuNP before and after the growth of the layer of silica, normalized at the stronger LSPR band of each system.

One can notice in the spectra presented in Fig. 1A and in the inset, a small redshift of around 2 nm in the LSPR band of AgNP at 438 nm with the coverage by the silicon oxide, as it would be expected for the SiO_2 ultrathin film formation over AgNP nanoparticles.[7] It is important noticing the increase in the absorption for longer wavelengths with the reaction time, and after two hours of reaction, no further increase in this feature is observed. The AuNP spectrum presented in Fig. 1B presents the characteristic band of spheroidal AuNP at 538 nm. The LSPR band at 538 nm redshifts 4 nm after 1 h reaction with silicate, and this LSPR band reach a maximum redshift of 6 nm after 2 h of reaction. No additional shift of the LSPR band was observed for additional reaction times. An important feature also observed in Fig. 1B is the increase of a shoulder in the LSPR band, which can be observed after a few minutes of reaction and remains with a similar relative intensity throughout the reaction time. The increase in absorption by both Au and AgNP in the near-infrared during the coverage reaction indicates the partial aggregation of the gold nanoparticles during the silicon oxide shell formation.

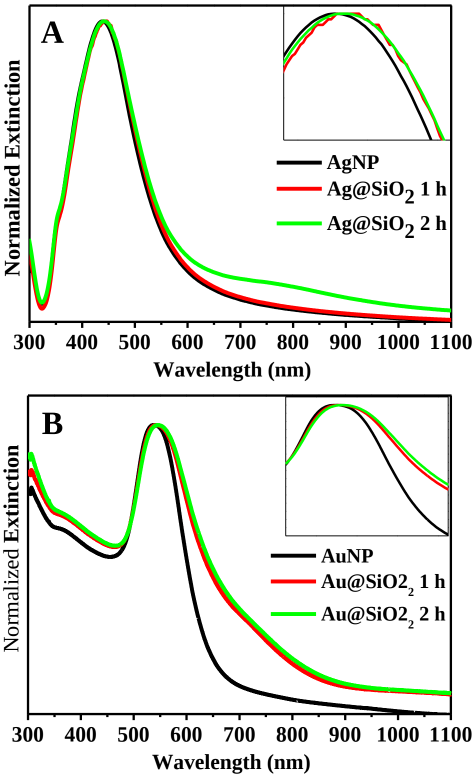

Figure 1. Extinction spectra: (A) AgNP and Ag@SiO$_2$ for different times of reaction; (B) same as A, but for AuNP. The inset in both figures shows a zoom-in to the maximum extinction of the nanoparticles suspensions.

Both Ag and Au@SiO$_2$ have been characterized by TEM. Figure 2 presents representative TEM micrographs for the AgNP (Fig. 2A) and AuNP (Fig. 2B) protected by silica layer, and additional TEM micrographs are presented in the Supporting Information. The TEM micrographs in Figure 2 clearly indicate the formation of an oxide layer (low contrast, blurry layer covering the Ag or Au nanoparticles). Indeed, that affirmation is confirmed by the chemical analysis, as can be seen in the EDX spectra shown on the insets of Fig. 2. The EDX spectra were acquired on STEM mode, with the focused electron beam positioned on the marked points in the figures. The micrographs presented in Figure 2 have been obtained for reactions times of 90 min; the thickness of the silica layer over the metallic nanoparticles is not homogeneous over the entire nanoparticle. The roughness is more evident for Ag@SiO$_2$ nanoparticles, as it can be more clearly seen in Figure 2A. There is no evidence of pinholes in the silica layer over any of the coinage metal nanoparticles, but it should be emphasized that TEM results are not conclusive about the presence of pinholes; however, the TEM images of the samples of several shell-isolated nanoparticles for both Ag@SiO$_2$ and Au@SiO$_2$, presented in Figs. S1 and S2 (see Supporting information) indicate that silica layer over the metallic particles has been observed without noticeable evidence of holes. Measurements in several nanoparticles indicate that the minimum SiO$_2$ thickness is at least 0.5-1 nm over the entire particle, and that the silica layer average thickness is about 3-4 nm for Ag@SiO$_2$ and 4-5 nm range for Au@SiO$_2$. One can notice from the TEM images in Fig. 2, S1 and S2 (see Supporting Information) that the size and shape vary considerably for the SHIN in the present work. This variability reflects the metallic nanoparticles preparation procedures used, which are simple and well-known; however, even with such wide size and shape variability, the SHIN prepared have presented silica coverage no matter what the size and shape of the metallic nanostructure are present in the samples. The SHIN of Ag@SiO$_2$ and Au@SiO$_2$ have been used as SHINERS and SHINEF substrates for a cyanine dye, IR-820, as discussed in the sections below.

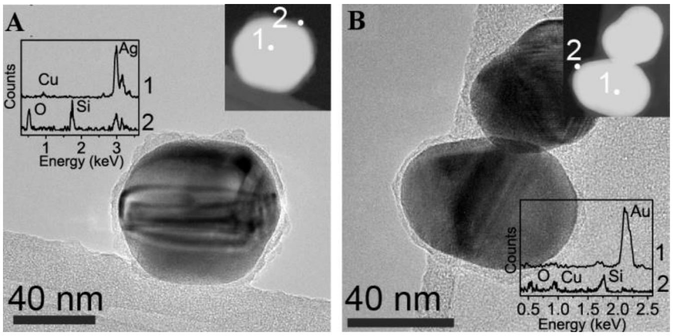

Figure 2. TEM micrographs of M@SiO$_2$, where: in A and B, M = Ag. Saturated HAADF images of the same particles are shown on the inset as well as the spectra collected on the outlined points. The micrographs have been obtained for M@SiO$_2$ obtained after 90 min growth of the ultrathin layers.

3.2. SHINERS of IR-820 on Ag@SiO$_2$ or Au@SiO$_2$ at 1064 nm

The as-synthesized M@SiO$_2$ nanoparticles (M = Ag or Au) have been separated from excess silica by centrifugation before it could be employed as SHINERS substrate. The probe molecule used has been the cyanine dye IR-820, and the SHINERS spectra were excited at 1064 nm; Figure 3 presents the results for both Ag@SiO$_2$ and Au@SiO$_2$. The Raman spectrum of an aqueous solution of IR-820 at the same concentration and spectral conditions is also presented for comparison purposes.

One can observe in Figure 3 an increase in Raman intensity of the probe molecule bands by several times in the presence of the M@SiO$_2$ nanoparticles, but the apparent enhancement in Raman intensities for the Ag@SiO$_2$ is much larger than for

$Au@SiO_2$. The calculation of the SERS/SHINERS "analytical enhancement factor" (AEF), following equation (1)[19]:

$$AEF = \frac{I_{SERS}/c_{SERS}}{I_{Raman}/c_{Raman}} \qquad (1)$$

Where I_{SERS} and I_{Raman} are the measured SERS and Raman intensity of a selected band, and c_{SERS} and c_{Raman} are the solution concentration employed for SERS and Raman measurements, respectively. In the present work, the band at 943 cm^{-1}, assigned to the δCH mode of the delocalized linear chain of IR-820,[16] has been chosen for the calculation of AEF. The band at 943 cm^{-1} was chosen because it is one of the most enhanced bands for the dye.[16] Considering the above cited band, the calculation of AEF for both $Ag@SiO_2$ and $Au@SiO_2$ resulted, respectively, in values of 173 and 3.0 for the SiO_2 layer growth time of 1 h and 35 and ~1.2 for the growth time of 1.5 h. The preceding AEF values are to be taken cautiously, as there are several limitations in the calculation model, as it has been pointed out before in the literature.[19, 20] One of the most important limitation is that the AEF calculations do not take into account the actual amount of probe molecules adsorbed on the nanostructure, but instead assumes that all probe molecules contribute equally to the enhancement factor. In order to correct such limitation, it would be necessary to refer to adsorption data on IR-820, which are not available in the literature.

Nevertheless, even considering the simplicity of the AEF model, one can notice that for the $Ag@SiO_2$ there are 2 orders of magnitude of Raman enhancement for the thinner layer obtained with 1 h of silica layer growth. Because there is a clear variation in SHINERS AEF between $Ag@SiO_2$ and $Au@SiO_2$, the measured values for this simple methodology have been adopted so it could be useful for comparison in different experimental SERS setups, and because it is suitable for a dynamic substrate as the one studied in the present work.[20] The value of AEF for $Ag@SiO_2$ is much larger than for $Au@SiO_2$, for both layer growth times presented in Figure 3. The better performance of $Ag@SiO_2$ nanoparticles as SHINERS substrates may be due to several factors, but it should be noticed that a thicker layer of silica that has been formed over the AuNP in a similar reaction time. Although the thickness of silica layer is different between $Au@SiO_2$ and $Ag@SiO_2$ for the same silica deposition time, the comparison of AEF has been performed for the same reaction time because it has been reported in the literature the striking dependence of the silica thickness on the reaction time.[1, 2] The larger value of the Quality Factor of plasmonic resonances for Ag compared to Au when excited at 1064 nm could also play a role in the AEF difference.[14] The larger value of QF for Ag reflects in the efficiency of electric field localization of the nanostructures, and therefore, in better SERS/SHINERS performance for Ag compared to Au.

The AEF measured for IR-820 adsorbed on $Ag@SiO_2$ are smaller than the ones measured for AgNP in a previous work,[16] but are in the same order of magnitude. The decrease in the AEF would be expected because the IR-820 molecules are in a larger distance from the nanoparticle surface on $Ag@SiO_2$ than in the case of AgNP, and the influence of the surface plasmon field enhancement is expected to be considerably smaller.

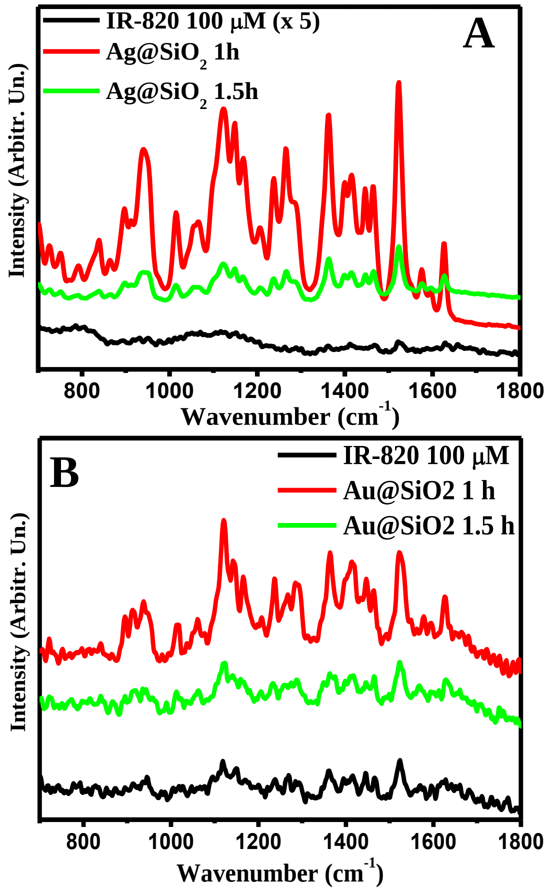

Figure 3. SHINERS spectra of IR-820 compared to the Raman spectra of IR-820 100 µmol L^{-1} in solution: (A) on $Ag@SiO_2$, using [IR-820] = 10 µmol L^{-1}; (B) on $Au@SiO_2$, using [IR-820] = 100 µmol L^{-1}. The spectra have been acquired for the dye adsorbed on SHIN obtained for 1 h and 1.5 h of reaction for the formation of the silica layer, as indicated in the figures. λ_0= 1064 nm.

It is worth mentioning that it has been predicted in computational results for nanospheres and nanospheres dimers that the SERS enhancement at 1064 nm should be small compared to other near-IR exciting wavelengths,[21] such as 785 and 832 nm; the decrease in performance would be due to larger losses caused by inhomogeneity in the oscillating dipole caused by the 1064 nm excitation compared to the other cited wavelengths. There are reports in the literature where the nanoparticle aggregation is used to improve the SERS performance of adsorbates on AgNP excited at 1064 nm.[22] In the present study, on the other hand, employing the SiO_2 ultrathin layer resulted in the avoidance of increase in the aggregation state of the nanoparticles caused by the adsorbate; this resulted in a lower AEF, but the SHIN/IR-820 suspension has been verified to be very stable for days, without solid deposition.

Additionally it should be noticed that no important shift in the band wavenumbers have been observed for the SHINERS results compared to the Raman of IR-820 in solution, which indicates a non-specific interaction between the dye and the silica surface. A similar result has been obtained in the SERS study of adsorption of IR-820 on Ag and Au nanoparticles,[16] as well as it has also been verified for indocyanine green (ICG), a structurally related cyanine dye, on gold.[23] On the other hand, one can observe a few changes in relative intensity between the IR-820 spectra on Ag@SiO$_2$ and on Au@SiO$_2$; one could notice that the intensity changes are subtle, and the signal-to-noise ratio for the spectra on Au@SiO$_2$ is much smaller than for Ag@SiO$_2$. The low signal may be responsible for those small changes in relative intensity, rather than important changes in the IR-820 interaction with the surface.

3.3. SHINEF of IR-820 on Ag@SiO$_2$ or Au@SiO$_2$ excited at 785 nm

The M@SiO$_2$ may present interesting conditions for the enhancement of fluorescence, as the silica layer may be able to keep fluorophores separated from the plasmonic nanoparticles by a few nanometers, which is an essential condition for plasmon enhanced fluorescence.[12] Previous reports on SHINEF have used mostly excitation in the visible region, especially in the green region of the visible spectrum.[6, 24, 25] Gold nanoparticles, on the other hand are expected to present high performance in plasmonic-based spectroscopies only in the red/near-infrared. Considering that silver nanoparticles also presented high performance in the near infrared, it has been employed IR-820 dye as SHINEF probe molecule for excitation at 785 nm. Figure 4 presents the comparison of the fluorescence spectrum of 1 μmol L^{-1} IR-820 aqueous solution to the spectrum of the dye in the presence of "bare" AuNP or AgNP, and in the presence of Ag@SiO$_2$ or Au@SiO$_2$ nanoparticles.

The AEF has been calculated for the SHINEF in the same manner used for the SHINERS results, and the values are presented in Figure 4 as well. One can notice that the difference in the AEF between Ag@SiO$_2$ and Au@SiO$_2$ is only *ca.* 6% for the excitation of IR-820 at 785 nm. The small difference between Au and Ag SHIN is most probably due to the use of 785 nm excitation, under which the LSPR quality factor is much closer for the coinage metals Ag and Au[14] than in the case of green excitation used in previous SHINEF experiments.[7] On the other hand, both enhancement factors measured in the present work are similar to those estimated from SHINEF reports in the literature for the dyes octadecyl-rhodamine-B and bis(n-butylimido)perylene excited at 514 nm.[6, 25] It is interesting noticing that a recent work by Osorio-Roman et al. report larger SHINEF enhancement factors, which has been obtained for aggregated Ag and Au SHIN nanoparticles,[26] which has been strongly depended on the aggregation state of the coinage metals nanoparticles.

It should also be emphasized that cyanine dyes with structures similar to IR-820, such as indocyanine green, tend to form dimers in aqueous solution for the concentrations used in the present work;[27, 28] taking this into account, the spectra of IR-820 in solution presented in Figure 4 is taken as the fluorescence spectrum of dimeric IR-820.

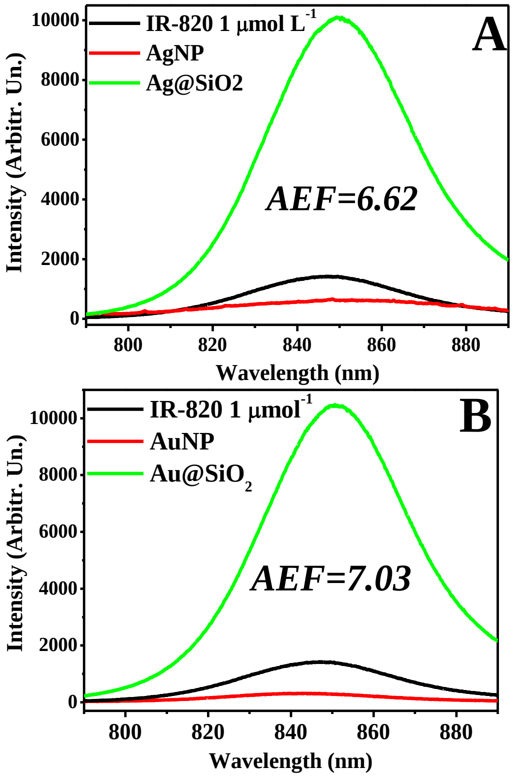

Figure 4. Fluorescence spectra of 1.0 μmol L^{-1} IR-820 in aqueous solution, in the presence of MNP and SHINEF on M@SiO$_2$, as indicated in each item; (a) Ag and (b) Au. λ_0=785 nm.

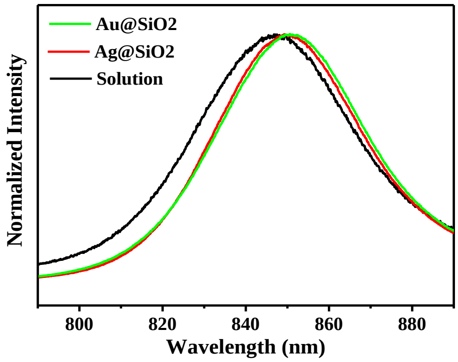

Figure 5. Normalized fluorescence spectra of 1 μmol L^{-1} IR-820 in solution, and on Au@SiO$_2$ and Ag@SiO$_2$, as indicated. λ_0= 785 nm.

Figure 5 presents fluorescence spectra of IR-820 in solution and on SHIN nanoparticles, normalized at the emission maxima, in order to understand the spectral changes for the dye. In Figure 5 one can notice a shift of maximum emission of IR-820 from 847 nm to 850 nm (on Ag@SiO$_2$) and 851 nm (on Au@SiO$_2$), together with a slight decrease in the FWHM of the fluorescence spectra from solution to the Ag@SiO$_2$ and Au@SiO$_2$ of 4% and 3%, respectively. The spectral changes are small compared to what would be expected if the aggregation state of the dye had changed in the presence of the nanoparticles. Those slight changes In FWHM are more likely to be assigned to a decrease in the mobility of the IR-820 dimer on the SHIN compared to the mobility of the dye in solution.

4. Conclusions

The present work presented the SHINERS and SHINEF effects of the dye IR-820 excited in the near-infrared, at 1064 nm and 785 nm, respectively. The plasmon enhanced effects have been obtained for Au@SiO_2 and Ag@SiO_2 SHIN.

The performance of Ag@SiO_2 for SHINERS excited at 1064 nm was considerably larger than for Au@SiO_2, which could be attributed to the larger quality factor value for Ag compared to Au even at 1064 nm. The overall performance of the Ag@SiO_2 is considerably lower than for the visible region of the spectra, and the conjunction to the cyanine dye IR-820 is essential for the observation of SHINERS. The M@SiO_2@IR-820 (M = Ag or Au) systems are stable in suspension and they could be applied for additional modifications.

The SHINEF performance for both Au@SiO_2 and Ag@SiO_2 SHIN in the presence of IR-820 excited at 785 nm is quite similar, different of what has been observed for excitation with green lasers, excitation in which the Ag@SiO_2 performs considerably better than Au@SiO_2. Similar performance of both coinage metal SHIN is assigned to the similar values of quality factor at 785 nm excitation.

The present work has, thus, presented the observation of silica based SHIN for enhanced spectroscopies in the near-infrared using a cyanine based dye as probe molecule.

Acknowledgements

The authors thank CNPq, FAPEMIG, UFJF and "Rede Mineira de Química" (RQ-MG–FAPEMIG) for financial support. GFSA thanks CNPq for a research fellowship. TBVN thanks CAPES for a fellowship.

Notes and references

[a] Laboratório de Nanoestruturas Plasmônicas, Núcleo de Espectroscopia e Estrutura Molecular, Departamento de Química, Universidade Federal de Juiz de Fora, R. José Lourenço Kelmer, s/n, Campus Universitário, 36036-900, Juiz de Fora, Brazil. * Corresponding author: gustavo.andrade@ufjf.edu.br ; Phone: +55(32)21023310.

[b] Divisão de Metrologia de Materiais, Instituto Nacional de Metrologia, Qualidade e Tecnologia (INMETRO), Av. Nossa Senhora das Graças, 50, Prédio 3, 25250-020, Duque de Caxias, Brazil.

Electronic Supplementary Information (ESI) available: Additional TEM micrographs of Au@SiO_2 and Ag@SiO_2. See DOI: 10.1039/b000000x/

1. J. F. Li, Y. F. Huang, Y. Ding, Z. L. Yang, S. B. Li, X. S. Zhou, F. R. Fan, W. Zhang, Z. Y. Zhou, D. Y. Wu, B. Ren, Z. L. Wang and Z. Q. Tian, *Nature*, 2010, **464**, 392-395.
2. J. F. Li, X. D. Tian, S. B. Li, J. R. Anema, Z. L. Yang, Y. Ding, Y. F. Wu, Y. M. Zeng, Q. Z. Chen, B. Ren, Z. L. Wang and Z. Q. Tian, *Nature Protocols*, 2013, **8**, 52-65.
3. V. Uzayisenga, X. D. Lin, L. M. Li, J. R. Anema, Z. L. Yang, Y. F. Huang, H. X. Lin, S. B. Li, J. F. Li and Z. Q. Tian, *Langmuir*, 2012, **28**, 9140-9146.
4. J. R. Anema, J.-F. Li, Z.-L. Yang, B. Ren and Z.-Q. Tian, *Annual Review of Analytical Chemistry*, 2011, **4**, 129-150.
5. P.-P. Fang, J.-F. Li, X.-D. Lin, J. R. Anema, D.-Y. Wu, B. Ren and Z.-Q. Tian, *Journal of Electroanalytical Chemistry*, 2012, **665**, 70-75.
6. A. R. Guerrero and R. F. Aroca, *Angewandte Chemie-International Edition*, 2011, **50**, 665-668.
7. A. R. Guerrero, Y. Zhang and R. F. Aroca, *Small*, 2012, **8**, 2964-2967.
8. R. F. Aroca, *Physical Chemistry Chemical Physics*, 2013, **15**, 5355-5363.
9. G. J. Kovacs, R. O. Loutfy, P. S. Vincett, C. Jennings and R. Aroca, *Langmuir*, 1986, **2**, 689-694.
10. N. P. W. Pieczonka and R. F. Aroca, *Chemphyschem*, 2005, **6**, 2473-2484.
11. T. W. Ebbesen, H. J. Lezec, H. F. Ghaemi, T. Thio and P. A. Wolff, *Nature*, 1998, **391**, 667-669.
12. J. R. Lakowicz, C. D. Geddes, I. Gryczynski, J. Malicka, Z. Gryczynski, K. Aslan, J. Lukomska, E. Matveeva, J. A. Zhang, R. Badugu and J. Huang, *Journal of Fluorescence*, 2004, **14**, 425-441.
13. K. Aslan and C. D. Geddes, *Chemical Society Reviews*, 2009, **38**, 2556-2564.
14. E. C. Le Ru and P. G. Etchegoin, *Principles of Surface-Enhanced Raman Spectroscopy: and related plasmonic effects*, Elsevier, Amsterdam, 2009.
15. M. K. Fan, G. F. S. Andrade and A. G. Brolo, *Analytica Chimica Acta*, 2011, **693**, 7-25.
16. T. B. V. Neves and G. F. S. Andrade, *Journal of Spectroscopy*, 2015, **2015**, 9.
17. G. Frens, *Nature-Physical Science*, 1973, **241**, 20-22.
18. P. C. Lee and D. Meisel, *Journal of Physical Chemistry*, 1982, **86**, 3391-3395.
19. E. C. Le Ru, E. Blackie, M. Meyer and P. G. Etchegoin, *Journal of Physical Chemistry C*, 2007, **111**, 13794-13803.
20. D. C. Rodrigues, M. L. de Souza, K. d. S. Souza, D. P. dos Santos, G. F. S. Andrade and M. Temperini, *Physical Chemistry Chemical Physics*, 2015.
21. M. G. Blaber and G. C. Schatz, *Chemical Communications*, 2011, **47**, 3769-3771.
22. H. Bengter, C. Tengroth and S. P. Jacobsson, *Journal of Raman Spectroscopy*, 2005, **36**, 1015-1022.
23. J. Kneipp, H. Kneipp, W. L. Rice and K. Kneipp, *Analytical Chemistry*, 2005, **77**, 2381-2385.
24. R. F. Aroca, G. Y. Teo, H. Mohan, A. R. Guerrero, P. Albella and F. Moreno, *Journal of Physical Chemistry C*, 2011, **115**, 20419-20424.
25. G. Moula and R. F. Aroca, *Analytical Chemistry*, 2011, **83**, 284-288.
26. I. O. Osorio-Román, A. R. Guerrero, P. Albella and R. F. Aroca, *Analytical Chemistry*, 2014, **86**, 10246-10251.
27. D. L. Akins, S. Ozcelik, H. R. Zhu and C. Guo, *Journal of Physical Chemistry A*, 1997, **101**, 3251-3259.
28. R. Philip, A. Penzkofer, W. Bäumler, R. M. Szeimies and C. Abels, *Journal of Photochemistry and Photobiology A: Chemistry*, 1996, **96**, 137-148.

Table of contents:

Graphical Abstract:

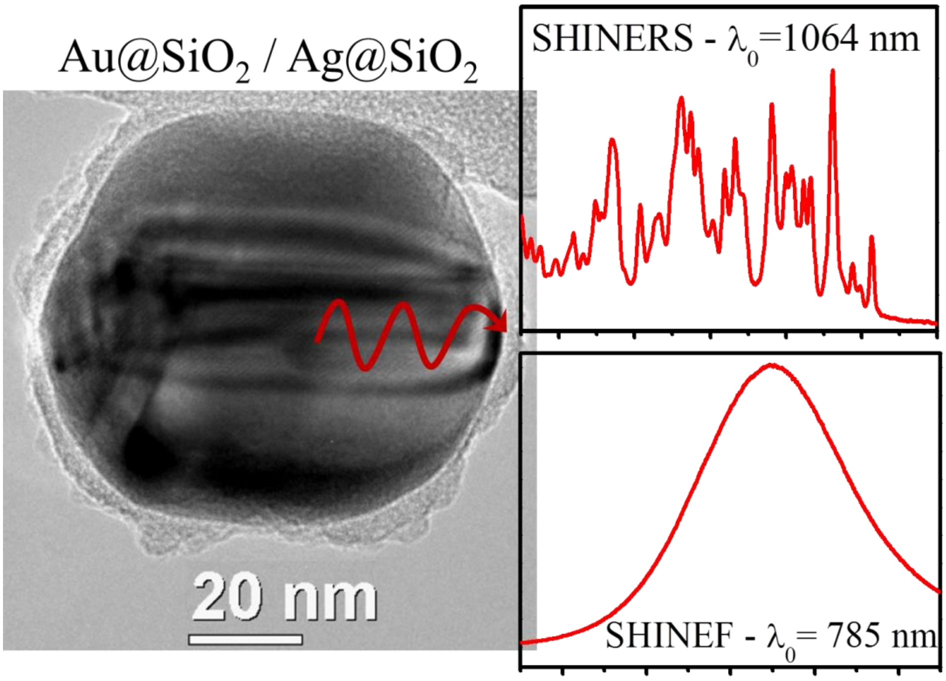

Textual Abstract:

SHINERS and SHINEF from $Ag@SiO_2$ and $Au@SiO_2$ excited in the near-infrared are presented, with high enhancement factors, together to TEM/EDX evidences of silica coverage over Au and Au nanoparticles.